AUTONOMOUS MOBILE DIRECTIONALLY AND SPECTRALLY SENSITIVE NEUTRON DETECTORS

R.J. GOLDSTON
Princeton University / Princeton Plasma Physics Laboratory
Princeton, NJ, USA
Email: goldston@pppl.gov

A. GLASER
Princeton University
Princeton, NJ, USA

M. KÜTT
Princeton University
Princeton, NJ, USA

P. LANDGREN
Princeton University
Princeton, NJ, USA

N.E. LEONARD
Princeton University
Princeton, NJ, USA

Abstract

The paper examines the potential of swarms of autonomous, mobile, directionally and spectrally sensitive neutron detectors ("Inspector Bots") to facilitate efficient and effective IAEA inspections. The inspection scenarios under consideration are 1) detection of undeclared withdrawal stations in the centrifuge halls of gas-centrifuge enrichment plants and 2) detection of the introduction of low-enriched UF_6 at feed stations in such plants. A preliminary light-weight gamma inspector bot has been constructed, carrying three miniature Geiger-Müller counters, for the purpose of prototyping search algorithms and intra-swarm communication. It has been shown to be capable of detecting check sources in the laboratory. The concept for a directional neutron detector in the form of a two-foot high, 8" diameter cylinder of polyethylene moderator, containing three boron-coated-straw neutron counters at a radius of 3", located 120° apart, is presented. This detector can be integrated onto a medium-capacity robot with Mecanum wheels for arbitrary direction of motion, including rotation. MCNP studies show that such a detector system provides both high sensitivity and directionality, making it practical for robot swarms to survey a large cascade hall for undeclared withdrawal stations during a Limited Frequency Unannounced Access, and for robotic Unattended Monitoring Systems to detect the introduction of low-enriched UF_6 in declared feed stations before a fraction of a Significant Quantity of highly enriched UF_6 is produced. The ratio of signals in the three detectors also provides neutron spectral information, making it possible to detect the presence of shielding. It is planned to test the sensitivity of the neutron detector, the stability of its directional indication, and its ability to detect shielding using a moderated and unmoderated ^{252}Cf source.

1. INTRODUCTION

IAEA inspections at declared nuclear facilities are constrained by the needs to 1) avoid exposure of sensitive information, 2) minimize impacts on facility operations, and 3) conserve inspectorate resources. We are examining the potential of swarms of autonomous, mobile, directionally and spectrally sensitive radiation detectors ("Inspector Bots") to facilitate efficient and effective inspections, expanding the capabilities of inspectors while remaining consistent with these requirements. Our robots are targeted to address two distinct scenarios:

1.1. Scenario 1: Clandestine HEU production in a Gas-Centrifuge Enrichment Plant (GCEP)

If only about 0.8% of the low-enriched UF_6 ($LEUF_6$) product of a 500 tSWU/a cascade hall were diverted to a small subset of the centrifuges in the hall, ideally 0.3% but practically more, and these centrifuges were configured to produce highly enriched UF_6 ($HEUF_6$), 1 SQ of 90% enriched $HEUF_6$ would be produced per year. The $HEUF_6$-producing centrifuges would generate tails with 0.71% enrichment to be sent back into the feed stream

of the plant. The overall mass balance of the plant would be off by only 0.003% and the ^{235}U balance by only 0.4%, making this is a very difficult scenario to detect by material balance accountancy alone. It does require significant re-plumbing of a small fraction of the centrifuges, and of central interest here, the $HEUF_6$ product would need to be withdrawn. The least conspicuous approach to withdrawal could be to replace the rotor inside one of the thousands of centrifuge casings with a withdrawal cylinder. For example, a 20 liter scuba cylinder with a diameter of 20 cm could hold 1 SQ of $HEUF_6$.

The main neutron source in UF_6 arises from the $^{19}F(\alpha, n)^{22}Na$ reaction due to α particles from spontaneous ^{234}U decay striking fluorine nuclei, with a smaller contribution from spontaneous fission of ^{238}U. ^{234}U enrichment tracks with the enrichment of ^{235}U in centrifuges, with a ratio rising from 0.76% for natural uranium to 0.95% for 90% enriched uranium.[1] [1]. As a result, (α, n) neutrons are produced (for 0.9% $^{234}U/^{235}U$ ratio) at the rate of 5082 n/s/kg ^{235}U [2] with an average energy of 1.1 MeV [3], while the production rate of neutrons from spontaneous fission is 26 n/s/kg ^{238}U, with an average energy of about 2 MeV. Thus neutron-detecting robots could search for anomalous neutron production from a "centrifuge" containing kilograms of ^{235}U, rather than the sub-gram quantities expected in centrifuges in even the most highly enriched stages under normal operation. It is unclear how often an operator would choose to replace a clandestine withdrawal cylinder, so it would be prudent to assume that much less than 1 SQ might be present at the time of a limited frequency unannounced access (LFUA). 1/10 SQ, or 2.5 kg of ^{235}U, contained in 90% enriched $HEUF_6$ produces $1.34\ 10^4$ neutrons per second.

1.2. Scenario 2: Rapid production of HEU in a GCEP

It is well known that the most rapid production of $HEUF_6$ in a GCEP involves feeding $LEUF_6$, rather than UF_6 containing only natural uranium ($NatUF_6$). A specific scenario for this, described in reference [4], shows that about 0.5 SQ of weapons-grade UF_6 can be produced per day in a 500 tSWU/a capacity cascade hall fed by $LEUF_6$, following minimal re-plumbing and minimal time for re-equilibration. In this scenario near real-time detection is essential, so unattended monitoring systems (UMSs) are required. As part of the re-plumbing activity, On-Line Enrichment Monitors (OLEMs) could be spoofed by plumbing the flow of $HEUF_6$ around them. The purpose of our approach is to render the entire set of feed stations at a large-scale GCEP unusable for feeding $LEUF_6$, necessitating a significant construction project for the implementation of this otherwise "rapid production" scenario. A 48Y UF_6 cylinder typically used for feed in GCEPs can hold up to 8.5 t of uranium, ~1% of the annual feed to our nominal cascade hall. Such a cylinder filled with 3% enriched $LEUF_6$ produces $1.42\ 10^6$ n/s, to be compared with $4.81\ 10^5$ n/s for a cylinder filled with $NatUF_6$. 48Y cylinders filled with $LEUF_6$ may be available in Product Blending Systems at GCEPs as "donor cylinders" for blending $LEUF_6$ of different enrichments to meet a customer's required enrichment [5]. Detectors would be tasked to measure the neutron field at each feed station and so determine if $LEUF_6$ were being fed into the cascade hall. Consultations indicate that this may be considered by operators as a service, because it would provide a check that donor cylinders were not accidentally placed in feed stations. Sensitivity to the neutron spectrum would provide information on whether feed cylinders were shielded to reduce their apparent neutron emission.

2. THE GAMMA MINI-INSPECTOR BOT

This robot serves as a versatile prototyping platform for search algorithms and intra-swarm communication. It uses small laboratory calibration gamma sources that can be handled easily in a University environment. We are currently not targeting it for application in Scenarios 1 and 2, since γ radiation is much easier to shield than neutron radiation.

The small robot, shown in Figure 1, is based on the ROBOTIS TurtleBot 3 Burger robot platform, occupying about one cubic foot. The platform includes an easily changeable geometry, motor controller, single-board computer (Raspberry Pi 3) and a small LIDAR sensor for distance measurements. Software provided by the manufacturer includes basic routines for navigation and simultaneous location and mapping (SLAM).

---

[1] Uranium reprocessed from used reactor fuel, uranium re-enriched from tails, or uranium downblended from HEU can violate these ratios, but should be detected when it is delivered to the enrichment plant.

To achieve directional sensitivity, we use three sensors on this robot, all on the outer surface with angles of 120° between them. The sensors are LND7317 pancake Geiger-Müller counters with high voltage (0.5kV) provided by three "iRover Boards" from International Medcom, Inc. The boards give a 3.3V logic pulse of approximately 130 µs length per detected event[2]. An Arduino Nano micro-controller is used to collect pulses from all three detectors and provides them as so-called "topics" in the Robotic Operation System (ROS) that is used to control the robot's movement and sensors.

Our initial manual-control tests with this robot show that it is capable of distinguishing sources with µCi strength from natural background at distances of up to two feet. The distance depends on the energy spectrum of the source; our tests were carried out using ^{60}Co and ^{22}Na sources. SLAM functionality is implemented; a first result of a map showing obstacles and radiation levels is given in Fig. 1.

FIG. 1. Image of gamma inspector bot searching room for gamma sources located under a mock warhead. Insets show (left) the occupancy map created using SLAM overlaid with the measured activity (red indicating higher activity) using estimated measurements given by Gaussian Process (GP) Regression (see Section 4) and (right) a larger view of the gamma inspector bot.

3. THE NEUTRON INSPECTOR BOT

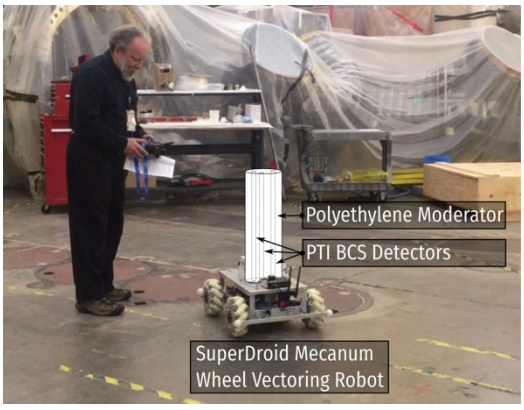

FIG 2. Neutron inspector bot under manual control by first author, whose height is 5' 5".

The proposed sensor to detect neutrons with high efficiency, good directionality, and sensitivity to neutron spectra, is comprised of three 1" diameter Proportional Technologies, Inc. Boron Coated Straw (BCS) counters embedded at a centerline radius of 3" in a cylindrical polyethylene moderator of 8" diameter, 120° apart. The BCS counters have similar performance to ^{3}He counters, absorbing thermal neutrons with high efficiency while remaining insensitive to gamma radiation. The SuperDroid Robotics IG52 DB vectoring robot provides a stable platform for the sensor, having the capacity to easily and safely maneuver a cylinder of polyethylene 24" high and 8" in diameter (Fig. 2) weighing 42 lbs. It is equipped with four Mecanum wheels, allowing the robot to drive in any direction and to rotate in place.

We first consider the sensitivity of our detector to neutrons in Scenario 1, the case of a hidden withdrawal station. Fig. 3 shows the count rate expected due to 2.5

[2] The same hardware is used by the Safecast Radiation Mapping project in their bGeigie nano device. https://blog.safecast.org/bgeigie-nano/

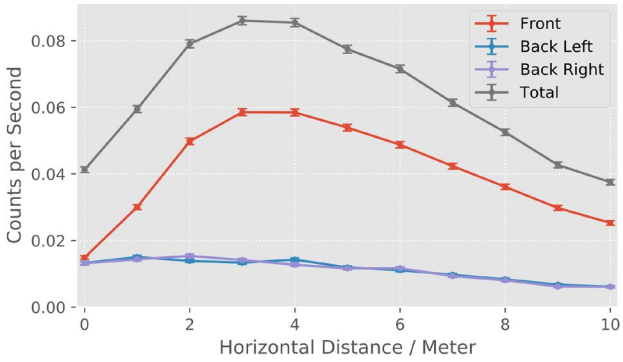

FIG 3. Total counts per second vs. horizontal distance from 90% enriched $HEUF_6$ sphere containing 2.5 kg ^{235}U elevated 5 m above detector midplane.

kg of ^{235}U contained in a sphere of 90% enriched $HEUF_6$, located vertically 5 m above the midplane of the detector, as a function of the horizontal distance between the $HEUF_6$ and the centerline of the detector. In this calculation we neglect absorption and scattering in the cylinder holding the $HEUF_6$ and in the surrounding centrifuges. The average total count rate over a 6.5 m radius circle where the withdrawal cylinder might be located is 0.078 cps, while the estimated background count rate is larger, at ~0.45 cps. A single stationary inspector bot can be used to provide a highly accurate time-averaged background count rate, which can also be compared with the time-averaged count rate of all of the inspector bots, since we do not expect many clandestine withdrawal stations.

With a goal of 2.28% for both the false positive and false negative rates, we set the detection threshold level for a selected measurement time at 2σ above background, corresponding to the required statistical false positive rate. Then we evaluate the false negative rate as a function of the horizontal distance from the clandestine withdrawal station to the detector (excluding a circle of radius 1 m above the detector, where a withdrawal cylinder could not be located), and average this over a selected area. We find that a counting time of 1350 seconds and an area of radius 6.5 m meets our 2.28%/2.28% goal. This corresponds to a swept area of 133 m^2 and a sweeping rate of 354 m^2/h. For a cascade hall of 3500 m^2 area, a survey would take five Inspector Bots only two hours. Thought of simply, there would be 26 independent survey areas, each with a 2.28% chance of a false positive, giving of an average of 0.6 false positives. These could be cleared quickly by the five robots. An optimized search algorithm should be able to do considerably better than this simple estimate, which neglects, for example, the directional information provided by the Inspector Bots. Fig. 4 shows the directional sensitivity of the detector at 5 m horizontal distance from the $HEUF_6$ sphere, elevated 5 m above the detector midplane.

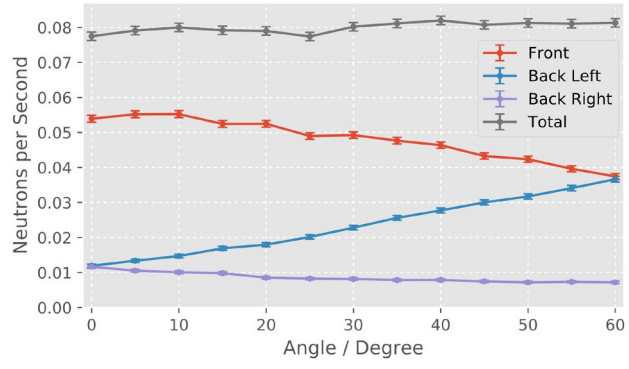

FIG 4. Counts per second in individual neutron counters vs. orientation to a hidden withdrawal station, elevated 5 m above detector midplane and 5 m horizontal distance.

For Scenario 2, we are interested in the Inspector Bot's response to neutrons emitted from UF_6 within 48Y cylinders. Fig. 5 presents results of MCNP simulations of total count rates in the Inspector Bot, due to neutrons emitted by a 48Y cylinder. The UF_6 is assumed here to form an annular layer on the inside of the cylinder. (An alternative configuration is considered in reference [6].) The detector was placed vertically, at a distance of 1.5 m between its surface and the front of a horizontal 48Y cylinder, with its midplane positioned 1.5 m below the midplane of the cylinder. We consider a range of fills levels, and $NatUF_6$, 3% enriched $LEUF_6$, and 5% enriched $LEUF_6$. Self-shielding of the neutron emission in

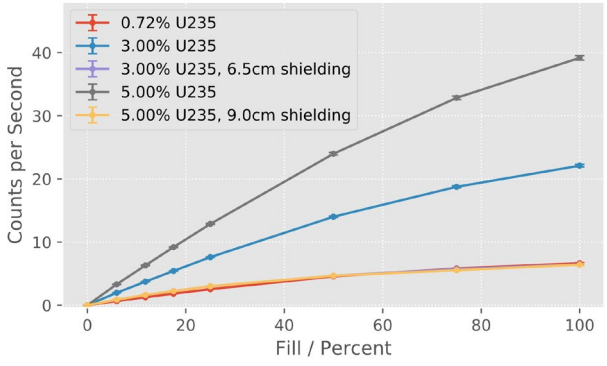

FIG 5. Total counts per second vs. enrichment. fill level and shielding with Inspector Bot 1.5 m in front of feed cylinder and 1.5 m below its centerline.

the UF_6 rises with increasing fill; this is partially compensated by neutron multiplication in the cases with higher enrichment.

An operator could choose to place neutron shielding around the outside of a 48Y cylinder filled with $LEUF_6$, in order to give count rates similar to $NatUF_6$. As shown in Fig. 5, a 6.5 cm shield of commercially available heat-resistant field-castable boron-silicone shielding wrapped around a 48Y UF_6 cylinder reduces the neutron counting efficiency by a factor of 3.4, enough to make a full cylinder of 3% enriched $LEUF_6$ produce a similar count rate to a full cylinder of $NatUF_6$. A 9 cm shield of the same material reduces the neutron counting efficiency by a factor of 6.1, enough to make a full cylinder of 5% enriched $LEUF_6$ produce approximately the same count rate. However, the neutron inspector bots are also sensitive to the hardness of the neutron spectrum, reflected by a change in the ratio between back (furthest from the source) and front counter rates, when the front counter is aligned towards the source. This is because a harder neutron spectrum penetrates the moderator more deeply. Fig. 6 shows that the back-to-front ratio is strongly affected by the shielding, which in addition to depleting the neutron spectrum, moderates it. In a single 15 minute measurement, the two cases are distinguishable to very high confidence.

An operator could instead put in place a 48Y cylinder initially 21.7% full of 3% enriched $LEUF_6$ or 12.5% full of 5% enriched $LEUF_6$, either of which would produce the same neutron count rate as nominal initial operation, as can be seen in Fig. 5. However, as shown in Fig. 6, such lightly filled cylinders would have dramatically different ratios of count rates in the front vs. back counters, as compared with nominal operation starting with cylinders filled with $NatUF_6$. This difference would be quickly detected. There may be a possibility, however, that an operator could add moderator (but minimal additional shielding) to the 48Y cylinder such as to cause the back-to-front ratio to track against the absolute count rate similarly to nominal operation, with a much reduced feed rate. If this proves to be possible, which is not certain, one could rotate the Inspector Bot to 30° to the centerline of the cylinder, making the problem even more difficult for an operator because the spectrum would be sampled differently in the left and right back counters, as seen for example in Fig 4. Ultimately the case of light fill with $LEUF_6$ could be detected by monitoring the UF_6 feed rate [7, 8], which would have to be much reduced to match the drop in total count rate vs. time.

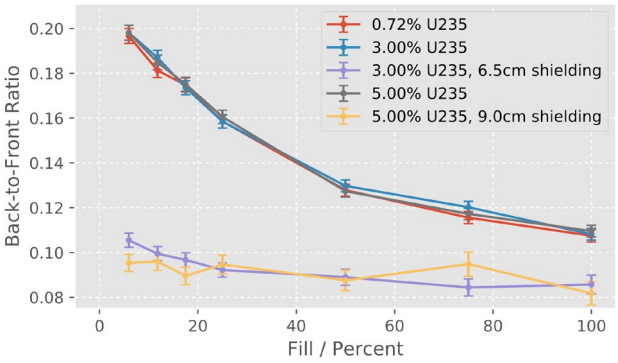

FIG 6. Back to front ratio vs. fill, enrichment and

4. SEARCH ALGORITHM DEVELOPMENT

In Scenario 1, Inspector Bots will face the dilemma of when to explore unsampled areas and when to continue measuring an existing location of interest. This core dilemma, of needing to explore an unknown environment, while also exploiting high-value locations, can be rigorously formulated using the multi-armed bandit (MAB) problem. We will use a variant of the MAB problem here to drive robot measurement behavior.

The MAB problem has been widely studied (see [9] for a review) and adapted for different scenarios. For example, it has been used to explain the foraging behavior of animals [10, 11]. Recently it has been investigated for designing decision-making and control in robotics [12, 13]. In the classical MAB problem, a decision-making agent chooses one from a set of options at each timestep. After choosing an option, the agent receives an associated reward, which may be stochastically variable. The agent's goal is to choose a sequence of options over time to maximize accumulated reward. The uncertainty in the reward returned for each option creates tension between choosing options that are known to return high reward (exploitation) versus options that are relatively unknown but with the potential to return even higher reward (exploration). Seminal work by Lai and Robbins [14] has demonstrated that there is a maximum achievable performance for MAB problems.

In the classical MAB problem, an agent will always try to identify the best option. An efficient alternative is the satisficing MAB problem [15], where an agent will only try to identify options with rewards that are above a threshold. We will use the satisficing formulation to guide our Inspector Bots in finding areas where the radiation

level is above a defined threshold. In the case of more than one Inspector Bot and means for them to communicate, we will leverage recent advances in the multi-agent MAB problem [16, 17, 18, 19]. In this setting, multiple agents make choices among the same set of options and share their information to explore the space of options more effectively.

4.1 Mapping

We will first use LIDAR-based SLAM to produce the occupancy map of the robot's surroundings. The occupancy map defines the area available for search: all unoccupied subareas (those without obstacles) that are a safe distance from an occupied subarea (those with obstacles) are deemed valid search locations. Host concerns will be taken into account as an overlay in defining valid search locations.

We then discretize the available search area into cells, and use Gaussian Process Regression to model the radiation field intensity and variance at each cell. For each cell we record the detector count events and dwell-time. Gaussian Processes (GP's) are widely used for estimating measured variables in adaptive sampling techniques [20], and are relatively computationally tractable when compared to other Bayesian techniques. They also allow for explicit characterization of correlation between cell locations. GP's have a long history in spatial measurement tasks such as oil well identification [21] and radiation measurements [22]. Researchers have also extended the formulation to incorporate gradient information [23], which can be used with the output from our neutron Inspector Bot.

4.2 Search

We will use a modified version of the (M, δ)-Satisficing Upper Confidence Limit (UCL) algorithm in [12] to perform efficient search over the area. The algorithm works as follows: For each valid cell *i* in the occupancy map, compute the value

$$Q_i(t) = \mu_i(t) + \sigma_i(t) + \Phi^{-1}\left(1 - \frac{\delta}{3}\right) \quad (1)$$

where $\mu_i(t)$ is the posterior estimate of the count rate at cell *i* as given by the GP, $\sigma_i(t)$ is the posterior standard deviation at cell *i*, $\Phi^{-1}(\cdot)$is the inverse Gaussian cumulative distribution function, and $\delta \in (0,1]$ is a certainty parameter. The robot then selects all cells with $Q_i(t)$ greater than threshold parameter M, and travels to the nearest of these cells. Additionally, if the measurement at cell *i* is above M by a given confidence margin, cell *i* is considered to be "known" and removed from the available set of cells.

$Q_i(t)$ is designed to send the robot to cells that are "optimistically" believed to have activity levels above M. The first term, $\mu_i(t)$, drives the robot to "exploit" locations that have relatively high measured activity levels, and the second term pushes the robot to "explore" locations with high uncertainty. The robot will then incrementally move across a space, investigating promising areas of high measured activity but also exploring poorly sampled areas.

In certain detection scenarios there may be additional information regarding the structure of the search space. For example, in a centrifuge hall the uniform, hallway-like nature of the space motivates designing into the robot's search algorithm additional logic for selecting which row to investigate. The modified UCL algorithm here can then be used during row traversal.

4.3 Multi-agent Search

The modified UCL algorithm can be expanded to multiple agents (Inspector Bots) with minimal modification. In this setting the robots share information regarding their measurements, location, and next sample point, and update their GP estimates independently. Each robot then selects where to travel as before, but eliminates or switches targets with another agent that is traveling to the same cell. This formulation has the benefit of being distributed and also robust to communication failures. Robots can be distributed over the space through their initial locations, but they will naturally convene to cover regions of interest.

5. FUTURE PLANS

In the case of the gamma mini-Inspector Bots, we plan to prototype both search algorithms and intra-swarm communication. In the case of the neutron inspector bots we plan to work with Proportional Technologies Inc., to build a single prototype neutron Inspector Bot. We will calibrate and test the prototype in a large shielded test cell at the Princeton Plasma Physics Laboratory, using a ^{252}Cf source. This source will be presented bare, or through 2.5" of polyethylene moderator, which will permit tests of the response of the detector to spectral hardness. We will calibrate the efficiency of the detector system as well as its angular resolution. We will also study the effect of large scattering objects, for example placing both the Inspector Bot and the ^{252}Cf source in the vicinity of a thick shield door, or other available massive metallic objects. All of these measurements will be compared with MCNP calculations.

The next step to support Scenario 1 is to undertake a survey of the background count rate in a large GCEP, to understand spatial and temporal variations in the signal, and how best to compensate them in order to minimize systematic uncertainties in the measurements.

As the next step for Scenario 2, we have proposed to bring a neutron Inspector Bot to a fuel fabrication facility, so that we can measure neutron production as a function of time while a 30B cylinder is drained of its $LEUF_6$. This will provide practical experience in a relevant environment, including other nearby feed cylinders and background gamma radiation.

6. CONCLUSIONS

We have found that relatively simple and robust autonomous, mobile, directionally and spectrally sensitive neutron detectors can provide a cost-effective means to enhance the effectiveness and efficiency of verification of gas centrifuge enrichment plants against both slow, clandestine production of $HEUF_6$ and also break-out to rapid $HEUF_6$ production. In the first case, they could detect a withdrawal station hidden within a large cascade hall during an LFUA. In the second, they could detect the feed of low-enriched uranium into a cascade hall, a signature of the fastest break-out scenarios, before a fraction of an SQ of $HEUF_6$ is produced.

ACKNOWLEDGEMENTS

This work supported in part by the National Nuclear Security Administration, U.S. Department of Energy, under contract DE-NA 0002534 for participation in the Consortium on Verification Technology, and by the U.S. Department of State Key Verification Assets Fund Award number SAQMMA17M1785.

The simulations presented in this article were performed using the Princeton Research Computing resources at Princeton University, which is a consortium of groups including the Princeton Institute for Computational Science and Engineering and the Princeton University Office of Information Technology's Research Computing department.

REFERENCES

[1] WOOD, H. G., Effects of separation processes on minor uranium isotopes in enrichment cascades, Science & Global Security, **16** 1-2 (2008) 26-36.

[2] SIMAKOV, S.P.,VAN DEN BERG, Q.Y., Update of the α − n Yields for Reactor Fuel Materials for the Interest of Nuclear Safeguards, Nuclear Data Sheets 139 (2017) 190-203.

[3] WILSON, W.B., PERRY, R.T., SHORES, E.F., CHARLTON, W.S., PARISH, T.A., ESTES, G.P., BROWN, T.H., ARTHUR, E.D., BOZOIAN, M., ENGLAND, T.R., MADLAND, D.G., STEWART, J.E., SOURCES 4C: A Code for Calculating (alpha,n), Spontaneous Fission, and Delayed Neutron Sources and Spectra, LA-UR-02-1839, Los Alamos National Laboratory, New Mexico/USA, 2002.

[4] WALKER, M.E., GOLDSTON, R.J., Timely verification at large-scale gas centrifuge enrichment plants, Science & Global Security **25** 2 (2017) 59-79.

[5] URENCO, National Enrichment Facility Safety Analysis Report, Revision 6, May 2005

[6] WALKER, M.E., GOLDSTON, R.J., GLASER, A., "Unattended 235U feed and withdrawal monitor for gas centrifuge enrichment plants", 58th Annual Meeting Institute for Nuclear Materials (Indian Wells, CA, 2017).

[7] GOLDSTON, R.J., KHODAK, A., JAWORSKI, M.A., SIBILIA, M.J., WALKER, M.E., "Unattended mass flow meter for gas centrifuge enrichment plants," 58th Annual Meeting Institute for Nuclear Materials (Indian Wells, CA, USA, 2017).

[8] WHITAKER, J.M., LAUGHTER, M., and HOWELL, J., "Using process load cell information for the IAEA safeguards at enrichment plants," IAEA-CN-184/116, IAEA Symposium on International Safeguards, (Vienna, Austria, 2010).

[9] BUBECK, S., CESA-BIANCHI, N., Regret analysis of stochastic and nonstochastic multi-armed bandit problems, Machine Learning **5** 1 (2012) 1–122.

[10] SRIVASTAVA, V., REVERDY, P., LEONARD, N.E., "On optimal foraging and multi-armed bandits", Allerton Conference on Communication, Control, and Computing (Monticello, IL, October 2013).

[11] KREBS, J.R., KACELNIK, A., TAYLOR, P., Test of optimal sampling by foraging great tits, Nature, **275** 5675 (1978) 27–31.

[12] SRIVASTAVA, V., REVERDY, P., LEONARD, N.E., Correlated and dynamic multiarmed bandit problems: Bayesian algorithms and regret analysis. In preparation.

[13] CHEUNG, M.Y., LEIGHTON, J., HOVER, F.S., "Autonomous mobile acoustic relay positioning as a multi-armed bandit with switching costs", IEEE/RSJ International Conference on Intelligent Robots and Systems (Tokyo, Japan, 2013).

[14] LAI, T.L., ROBBINS, H., Asymptotically efficient adaptive allocation rules, Advances in Applied Mathematics, **6** 1 (1985) 4–22.

[15] REVERDY, P., SRIVASTAVA, V., LEONARD, N.E., Satisficing in multi-armed bandit problems, IEEE Transactions on Automatic Control, **62** 8 (2017) 3788–3803.

[16] LANDGREN, P., SRIVASTAVA, V., LEONARD, N.E., "On distributed cooperative decision-making in multiarmed bandits", European Control Conference (Aalborg, Denmark, June 2016), arXiv preprint arXiv:1512.06888. to appear.

[17] LANDGREN, P., SRIVASTAVA, V., LEONARD, N.E., Distributed cooperative decision-making in multiarmed bandits: frequentist and Bayesian algorithms, arXiv:1606.00911 (2016).

[18] ANANTHARAM, V., VARAIYA, P., WALRAND, Asymptotically efficient allocation rules for the multiarmed bandit problem with multiple plays-part I: I.I.D. rewards, IEEE Transactions on Automatic Control, **32** 11 (1987) 968–976.

[19] SHAHRAMPOUR, S., RAKHLIN, A., JADBABAIE, A., "Multi-armed bandits in multi-agent networks", 2017 IEEE International Conference on Acoustics, Speech and Signal Processing (ICASSP), 2017. doi: 10.1109/icassp.2017.7952664.

[20] RASMUSSEN, C.E., WILLIAMS, C., Gaussian Processes for Machine Learning, MIT Press, Cambridge, MA (2008).

[21] DIGGLE, P., RIBEIRO, P.J., Model-based Geostatistics, Springer Science Business Media, LLC, (2010).

[22] WAINWRIGHT, H.M., SEKI, A., CHEN, J., SAITO, K., A multiscale Bayesian data integration approach for mapping air dose rates around the Fukushima Daiichi nuclear power plant, Journal of environmental radioactivity **167** (2017) 62–69.

[23] WU. A., AOJ, M., PILLOW, J., Exploiting gradients and Hessians in Bayesian optimization and Bayesian quadrature. arXiv:1704.00060 (2018).